ACS OMEGA

http://pubs.acs.org/journal/acsodf

Article

Surface Modification of Polytetrafluoroethylene Hollow Fiber Membrane for Direct Contact Membrane Distillation through Low-Density Polyethylene Solution Coating

Mohamad Razif Mohd Ramli, Abdul Latif Ahmad,* and Choe Peng Leo

Cite This: *ACS Omega* 2021, 6, 4609−4618

Read Online

ACCESS | Metrics & More | Article Recommendations

ABSTRACT: Membrane distillation (MD) is an attractive technology for the separation of highly saline water used with a polytetrafluoroethylene (PTFE) hollow fiber (HF) membrane. A hydrophobic coating of low-density polyethylene (LDPE) coats the outer surface of the PTFE membrane to resolve membrane wetting as well as increase membrane permeability flux and salt rejection, a critical problem regarding the MD process. LDPE concentrations in coating solution have been studied and optimized. Consequently, the LDPE layer altered membrane morphology by forming a fine nanostructure on the membrane surface that created a hydrophobic layer, a high roughness of membrane, and a uniform LDPE network. The membrane coated with different concentrations of LDPE exhibited high water contact angles of 135.14 ± 0.24 and 138.08 ± 0.01° for membranes M-3 and M-4, respectively, compared to the pristine membrane. In addition, the liquid entry pressure values of LDPE-incorporated PTFE HF membranes (M-1 to M-5) were higher than that of the uncoated membrane (M-0) with a small decrease in the percentage of porosity. The M-3 and M-4 membranes demonstrated higher flux values of 4.12 and 3.3 L m^{-2} h^{-1} at 70 °C, respectively. On the other hand, the water permeation flux of 1.95 L m^{-2} h^{-1} for M-5 further decreased when LDPE concentration is increased.

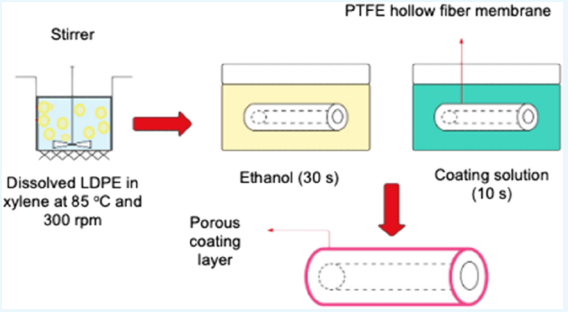

1. INTRODUCTION

Clean and freshwater are getting scarcer, and soon, most of the world population will be facing water-stressed conditions due to climate change, industrialization, and global increase in urbanization, all of which need urgent attention. To resolve the overarching issue, growing research interest in recent years has centered on the treatment of aquaculture of seawater through water purification technologies. The desalination of seawater has become an essential and promising option to meet the rising demand for clean water. Membrane technology is the most common separation method that can be classified into pressure-driven and non-pressure-driven processes depending on the separation mechanism. Desalination by reverse osmosis (RO) is a widely used technology for the removal of salts from feed water.[1] However, RO is operated under a high pressure, which requires high energy consumption.[2] Therefore, to address these limitations, membrane distillation (MD) is often proposed as an alternative technology because of its unique benefits associated with the process.[3] Membrane distillation (MD) is a thermally driven separation process associated with the membrane process. MD is an alternative to conventional distillation and RO separation, which is still in its testing stages and not fully applied within the industry.[4] Most researchers are interested about implementing MD in wastewater treatment, especially from the textile industry,[5] rubber industry,[6] mining industry,[7] and dairy industry.[8] MD is operated using a hydrophobic membrane to allow only vapor molecules rather than bulk water across the microporous membrane under lower pressure and lower operating temperature compared to RO and distillation, respectively.[9] Ideally, MD offers several advantages such as potential 100% rejection on nonvolatile dissolved substances,[10] productions of high-purity distillate, simple operation, easy to scale up, and relatively low energy consumptions.[11] In the present, the raw materials chosen for membrane fabrication for MD depend on their life spans, thermal stability, and chemical and mechanical resistance, in which most of the industrial processes use organic polymers and inorganic materials.[12] The MD process can be classified into four different configurations, which are direct contact membrane distillation (DCMD),[13,14] vacuum membrane distillation (VMD),[15] air gap membrane distillation

Received: October 20, 2020
Accepted: December 8, 2020
Published: February 9, 2021

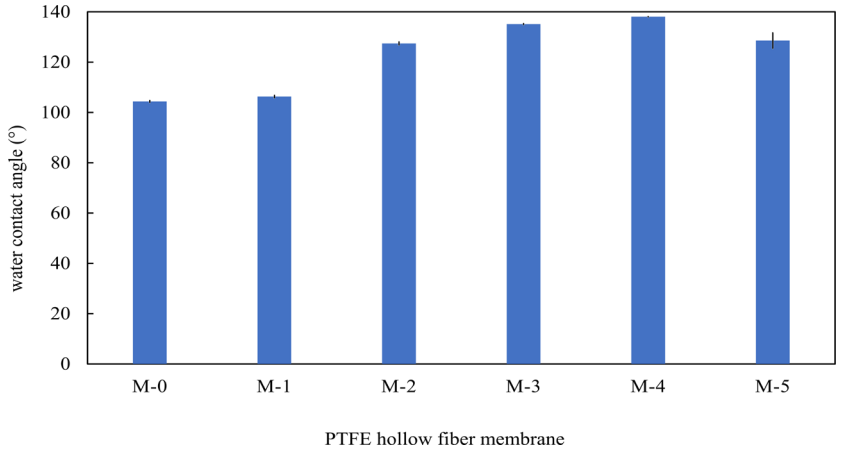

Figure 1. Water contact angle of PTFE HF membrane.

(AGM),[16] and sweep gas membrane distillation (SGMD).[17] Among those configurations, DCMD is one of the most common configurations used due to its simplest MD to treat concentrated wastewater.[18] For practical use, the membrane is the cornerstone of MD, which can exhibit long-term permeation flux and salt rejection. Despite the advantages of membrane distillation over conventional distillation, membrane wetting is the primary issue in desalination technologies by MD. To achieve efficient operation of the MD process, a superhydrophobic membrane is required to prevent pore wetting and penetration by liquid water.[19,20] Almost all industries use hydrophobic polymeric materials including polyethylene (PE), polypropylene (PP), polyvinylidene fluoride (PVDF), and polytetrafluoroethylene (PTFE).[21] Hydrophobic polymeric membranes that are made from PTFE and PVDF are commonly applied in MD.[22] The membrane is subjected to pore wettability with such high surface energy, which decreases membrane flux and rejection.[23] PTFE has a lower surface energy compared to PVDF, thus probably having a higher wetting resistance as well. Moreover, in comparison to PVDF with large pore size, the commercial PTFE membrane with smaller pore size is resistant to irreversible fouling, which might reduce the permeate flux and affect the performance of direct contact membrane distillation (DCMD).

One of the major obstacles limiting MD from commercialization in the industrial separation technology is the lower permeation flux compared to the pressure-driven membrane process due to fouling in water treatment and membrane wetting.[24] There are several parameters of the membrane to consider in improving the membrane performance and efficiency such as porosity, tortuosity, chemical resistance, thermal conductivity, and quality of distillate product. To satisfy this condition, first of all, the membrane must not be wetted by separate aqueous solutions and carry only water vapor through the membrane.[25] Also, suspended solids and organic matter are among the types of waste that can cause membrane blockage and increase the risk of membrane pore wetting. In addition, controlling the wetting of the membrane is one of the most significant obstacles in improving membrane efficiency and prolonging membrane life, as pore wetting typically leads to lower permeation flow due to the polarization effect of temperature (TPC).[26] This phenomenon occurs when a non-isothermal boundary layer is formed on both sides of the membrane surface. The temperature difference between liquid/vapor interfaces and the bulk phase is called temperature polarization, which has a destructive effect on the produced driving force and imposes resistance to heat transfer.[27] The development of a membrane with hydrophobic characteristics for the application of membrane distillation is therefore being considered.[28−30]

Surface modification is one of the proposed techniques to prevent membrane wetting by altering the morphology of the membrane surface. Modification of the membrane can be done by surface coating and grafting. Among those two methods, the coating of the membrane is the easiest approach to augmenting the hydrophobicity of the membrane by depositing the functional thin film layer on the outer surface of the membrane.[31] Many works have been done to develop porous and hydrophobic surfaces by a simple and inexpensive approach. Li et al.[32] and Chen et al.[33] described a simple solvent−nonsolvent coating method to prepare a lotus-like surface with superhydrophobic polyvinyl chloride (PVC). The membrane coating with PVC by Chen et al.[33] obtains a superhydrophobic porous surface with a water contact angle of more than 150°. In addition, porous superhydrophobic coating by low-density polyethylene (LDPE) has also been used to modify the membrane surface and successfully achieved a 152° water contact angle.[34] Similarly, Lu et al.[35] synthesized an LDPE superhydrophobic surface exceeding water contact angle of 173° by controlling the nucleation rate and adjusting the crystallization time. In addition, cooperative porous microstructures and floral crystal with a nanostructure of LDPE become favorable to enhance wettability resistance of the membrane. In view of this, by modifying the surface morphology through the process of producing hierarchical surface roughness, the hydrophobicity of the membrane could be altered. Thus, an attempt was made in this study on the modification of the PTFE surface via an LDPE coating solution for desalination.

2. RESULTS AND DISCUSSION

2.1. Effect of LDPE Concentrations. In this study, the effect of LDPE concentration in the coating solution on the hydrophobicity of the coated PTFE HF membranes by droplet water contact angle (WCA) was evaluated. All PTFE membranes exhibited a hydrophobic characteristic with a contact angle higher than 90°. Figure 1 shows that the surface WCA had an increase with a variation of (104.39 ± 0.38°), (106.30 ± 0.53°), (127.44 ± 0.62°), (135.14 ± 0.24°), and (138.08 ± 0.01°) for M-0, M-1, M-2, M-3, and M-4,

https://dx.doi.org/10.1021/acsomega.0c05107
ACS Omega 2021, 6, 4609−4618

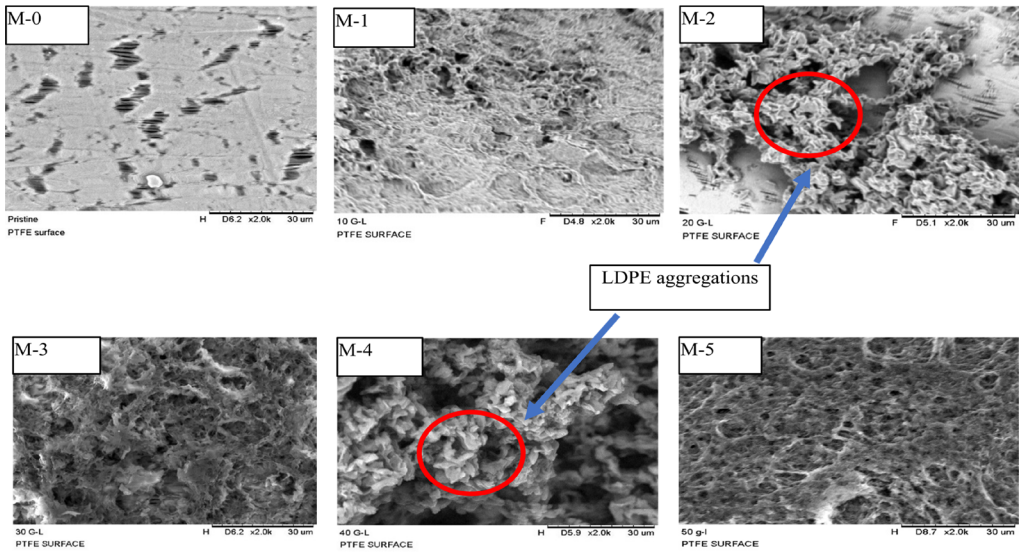

Figure 2. SEM images of coated and uncoated PTFE HF membranes.

respectively, with the gradual increase in LDPE concentration in the PTFE coating layer and a decrease about ±10° for M-5 at (128.58 ± 3.09°) due to poor solubility of LDPE in the coating solution at high concentration. In addition, higher LDPE concentration (50 g/L) promoted a higher solution viscosity, which affected the uniformity of the crystalline structure on the membrane surface. The high error of WCA for M-5 (±3.09°) among other membranes shows that the cracking of the LDPE layer may have occurred on certain surfaces of PTFE HF membrane and is responsible for the reduction of WCA. These findings suggest that PTFE layer coating and LDPE integration would increase PTFE HF membranes' surface hydrophobicity.

The water contact angle could be predicted by using the Wenzel equation:[36]

$$\cos \theta_w = R_f \cos \theta_o \quad (1)$$

θ_w and θ_o are the water contact angles upon the rough and smooth solid surface, respectively. R_f is the nondimensional surface factor, which is equivalent to the ratio of the surface area of its flat projected area. These Wenzel equation and Wenzel model illustrated that when the contact angle is $\theta > 90°$, the membrane is more hydrophobic. Surface roughness and non-wettability of the membrane material itself are two general factors affecting WCA surface hydrophobicity.[37] According to the figure above, the shape of the water droplets on the membrane is different from the pristine PTFE HF membrane (M-0) as compared to the PTFE coated layer due to the rough hydrophobic surface. Due to its low hydrophobicity, the high wetting rate occurred in pristine PTFE. Obviously, the PTFE surface roughness increased following the coating with LDPE, which promotes high wetting resistance due to the nano- and microstructure of the LDPE surface. Thus, the surface of LDPE−PTFE HF membranes can be better during MD.

2.2. Morphologies of Different PTFE HF Membranes. The LDPE coating solution is expected to modify the membrane surface. Figure 2 illustrates the surface morphologies for the SEM images of different PTFE HF membranes with 2000 magnifications. As shown, the membrane surface has a uniform topography and pore distribution for pristine PTFE (M-0), and major changes on the surface morphology of the membranes M-1, M-2, M-3, M-4, and M-5 have been observed. Under the coating method, SEM revealed that the uniformity of the formed LDPE layer has improved according to different concentrations of LDPE coated on the surface of PTFE membranes. The indirect coating method was based on the work from the literature,[32] which developed a rough LDPE layer that could facilitate an interfacial interaction between a solvent and nonsolvent on the surface of PTFE HF membrane, further causing tensions to shrink. Consequently, the flat interface of the coating layer was divided into various curved surfaces for M-3 and M-5 that resulted in precipitation of LDPE and microphase separation to take place on the surface of the membrane.[32] In addition, the fine nanostructure on the membrane surface was formed and created a hydrophobic layer, a high roughness of membrane, and a uniform LDPE network. In addition, M-4 exhibited fine and scattered LDPE aggregations on the membrane surface. As for M-1 and M-2, the lower concentration of LDPE coating solution left on the PTFE membrane surface was not adequate, resulting in the formation of a non-uniform coated layer, which correlated with the instability of the coating solution on the surface of the membrane. As a result, the incorporation of LDPE on the outer surface of the hollow fiber membrane is expected to effectively enhance membrane hydrophobicity and increase permeate flux during the MD process.[38]

2.3. Wetting Resistance of PTFE HF Membrane. Measurement of hydrophobic wetting resistance for the MD method is a significant criterion dependent on its contact angle as well as LEP.[39] The LEP value of the membrane in MD should be sufficient to avoid wetting. The LEP values for various PTFE HF membranes are shown in Figure 3. Compared to the pristine PTFE membrane, which was 0.2132 ± 0.01 bar, the LEP data for all coated PTFE HF membranes showed an increase from 0.2 to 0.99 bar. Obviously, the LEP values of the LDPE-incorporated PTFE HF membranes (M-1 to M-5) are higher than the uncoated membrane (M-0), as shown in Figure 3.

These results indicate that the PTFE HF membrane needs higher pressure to allow liquid across membrane pores and the PTFE coating layer effectively improves the wetting resistance

https://dx.doi.org/10.1021/acsomega.0c05107
ACS Omega 2021, 6, 4609−4618

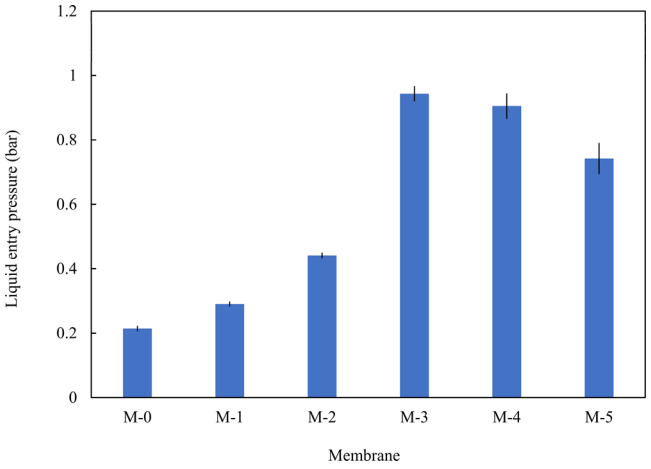

Figure 3. LEP of PTFE HF membranes.

of the hydrophobic PTFE HF membrane. In addition, the Laplace equation can be used to evaluate LEP values, which mainly depends on membrane hydrophobicity and pore structure[40,41]:

$$\mathrm{LEP} = \frac{-2B\gamma_1 \cos\theta_w}{r_{max}} \quad (2)$$

where the coefficients of B, γ_1,and θ_w refer to the pore geometric factor, liquid surface tension, and contact angle, respectively. r_{max} is the maximum pore size (radius), as that is the highest tendency to wetting. It is readily apparent from the equation that the LEP was found to vary from M-0 to M-5 due to the variations not only in surface water contact angle but also in the variance of surface topology and pore size distribution. After coating the PTFE HF membrane with the LDPE layer, the pore size was basically maintained and porosity remained around 58−62%. The values of porosity, contact angle, and LEP are listed in Table 1.

Table 1. Properties of PTFE HF Membranes

PTFE membrane	porosity (%)	contact angle (°)	LEP (bar)
M-0	62.45 ± 0.43	104.39 ± 0.38°	0.2132 ± 0.01
M-1	61.94 ± 0.07	106.30 ± 0.53°	0.2856 ± 0.01
M-2	60.55 ± 0.35	127.44 ± 0.62°	0.4502 ± 0.01
M-3	60.18 ± 0.10	135.14 ± 0.24°	0.9868 ± 0.02
M-4	59.01 ± 0.33	138.08 ± 0.01°	0.9945 ± 0.04
M-5	58.50 ± 0.37	128.58 ± 3.09°	0.8420 ± 0.05

Table 1 shows the trend of porosity with the increase in the LDPE concentrations (10−50 g/L). This indicates that the coating layer of LDPE does not block and penetrate the micropores of the PTFE HF membrane. However, M-4 has a high LEP and contact angle for resistivity to membrane wetting, but it is relatively lower in porosity compared to M-0. This phenomenon can be explained based on the Cassie−Baxter equation (CB, eq 3)[42]

$$\cos\theta_{CB} = rf_s \cos\theta_\gamma - f_v = f_s[r\cos\theta_\gamma + 1] - 1 \quad (3)$$

where θ_{CB}, θ_γ, and f_s and f_v are the apparent contact angle, the intrinsic contact angle on the original smooth surface, and the fractional areas of the solid and vapor on the surface, respectively. Based on the equation, the contact angle should be lower by decreasing the porosity at the higher LDPE concentration. However, it indicates that the membrane with a higher contact angle and LEP shows a decrease in porosity value, and hence, this phenomenon has a major impact on the vapor permeation of the MD phase.

2.4. Polymer Crystallinity. Polymer crystallinity by FTIR analysis was determined to investigate the influence of LDPE concentration on the changes in membrane chemical functional groups and crystal structure. Figure 4 shows the FTIR spectra result of the membrane. All PTFE HF membranes have C−F stretch at the 1400−1000 cm^{-1} wavenumber. There are two characteristic peaks for PTFE membranes at 1201 and 1146 cm^{-1}, which represent the CF2 asymmetric and symmetrical stretching bands, respectively.[43,44] Rocking and wagging vibration at 658 cm^{-1} was also found to be similar to the findings from the literature.[45−48] The LDPE-coated membranes M-1 to M-5 present elements of carbon (C) and hydrogen (H) with a long chain of CH_2 repeating unit.[49] The CH_2 asymmetrical and symmetrical stretching observed at wavenumbers 2915.98 and 2848.29 cm^{-1} recorded different intensities, which is also similar to the findings reported by Gulmine et al.[50]

2.5. DCMD Flux Performance. Figure 5a−c shows the DCMD flux performance of different PTFE HF membranes in sodium chloride and distilled water as a feed, final conductivity, and salt rejection. It can be seen from Figure 5a,b that the tested membrane samples demonstrated various permeation flux values because of the significantly different surface hydrophobicity, LEP, and porosity after undergoing surface modifications. It is important to note at this stage that all membranes have been able to maintain 99% of sodium chloride (NaCl) content in feed with different values of permeate conductivity at the end of the performance test. These high rejection values have shown that the LDPE hydrophobic coating on the surface of the membranes only permitted water vapor to be transported via microporous membranes. The final conductivity values of all modified membranes show excellent improvement in the range of 6.819−49.32 μS compared to the pristine PTFE HF membrane at 285.94 μS. The higher value of conductivity for the pristine PTFE HF membrane could suffer for long operation hours of DCMD and contribute to lower NaCl rejection. Using different concentrations in membrane modification, M-0, M-1, M-2, M-3, M-4, and M-5 membranes exhibited a difference in performance in terms of permeate flux. The LDPE coating layer on the outer surface of the PTFE HF membrane (M-1 to M-5) excellently enhanced the permeation flux of the pristine PTFE membrane (M-0). Permeate flux of M-0 membrane was the lowest for distilled water and NaCl ranging between 0.0023 and 0.0026 L m^{-2} h^{-1} and between 0.0013 and 0.0014 L m^{-2} h^{-1}, respectively, after 6 h. The incorporation of LDPE in the coating of the PTFE layer achieved higher permeate flux of distilled water and NaCl (4.36−5.08 and 3.84−4.12 L m^{-2} h^{-1}), respectively, compared to the permeate flux of M-1, M-2, M-4, and M-5 membranes. These results confirm that enhancement of surface hydrophobicity for the modified M-3 membrane at an optimum concentration of LDPE coated on the outer surface effectively improves membrane water flux. The water contact angle increased from 104.39 to 138.08°, the LEP value increased in the range 0.2−0.99 bar, and the deposition of a polymeric porous superhydrophobic thin layer on the outer surface of PTFE HF membrane with an acceptable range value of porosity about 60% has contributed to better permeation in

https://dx.doi.org/10.1021/acsomega.0c05107
ACS Omega 2021, 6, 4609−4618

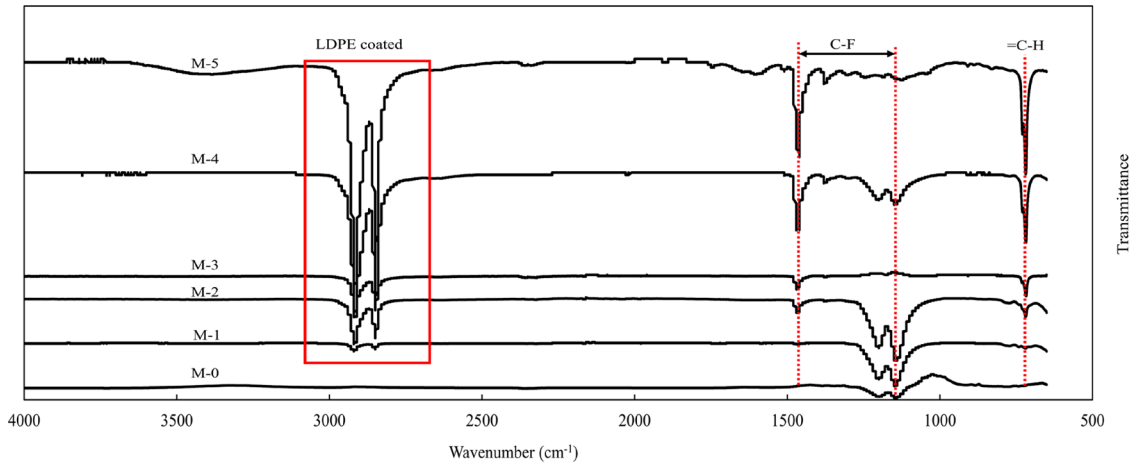

Figure 4. FTIR spectra of coated and uncoated PTFE HF membranes.

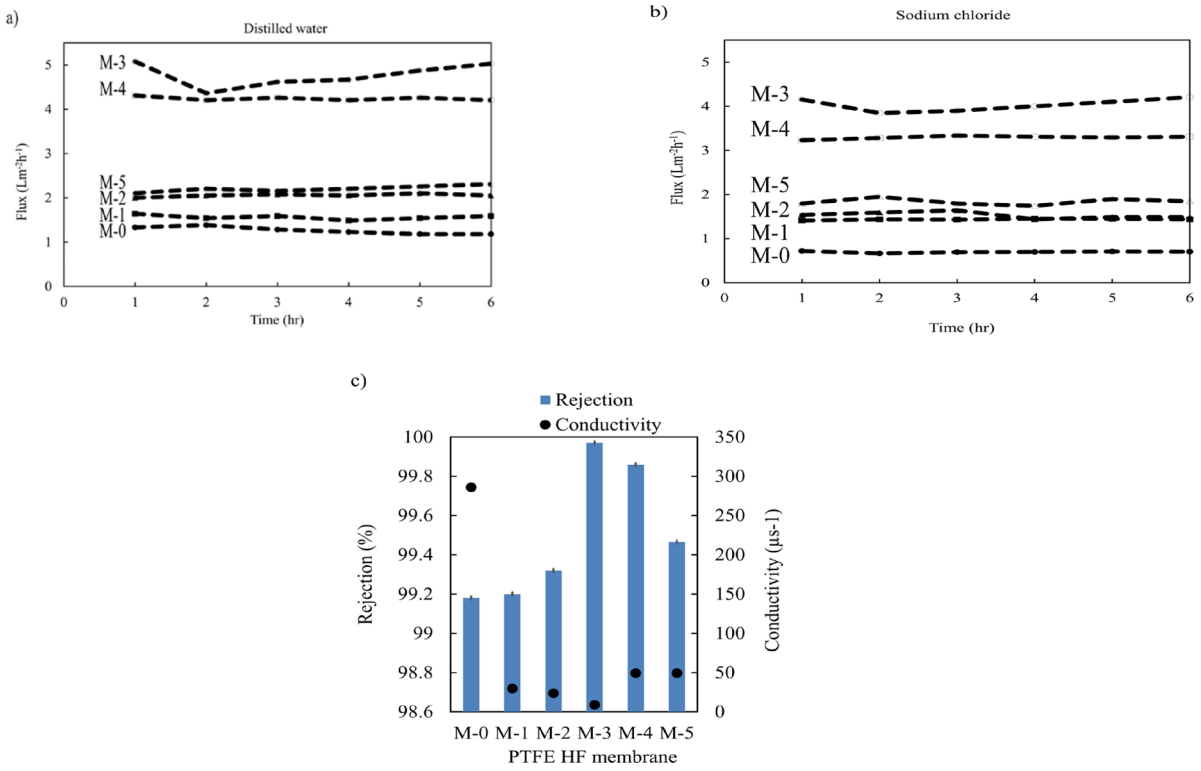

Figure 5. Water permeation flux for (a) distilled water and (b) sodium chloride. (c) Rejection and conductivity of different PTFE membranes.

the practical application of MD. Therefore, the optimum concentration of LDPE solution did not penetrate the membrane pores until a further increase in concentration, which leads to a reduction of membrane flux. In addition, Rosli et al.[51] tested the performance of pristine and LDPE-coated membranes to evaluate the effect created by the super-hydrophobic layer by LDPE solution coating. Based on Rosli et al.'s investigation, in different applications, the flux of the modified membrane is twice the flux of the pristine PVDF membrane. On the other side, a further increase in LDPE concentration on the membrane has shown the reduction of flux values for modified M-4 and M-5 about 21.45 and 54.76%, respectively. The thickness of the coating layer on the surface of the membrane could be a main contributor to the increased mass transfer resistance. Thus, the permeation flux outcomes exhibited good agreement with the characterization results.

Table 2 presents the summary of works demonstrating the advantages of the modified membrane in this study over the membranes in other works in terms of membrane properties and performances.

The LDPE−PTFE HF membrane mass transfer diagram is shown in Figure 6 to demonstrate the effect of the LDPE coating layer during the MD performance test on the mass transfer of the PTFE HF membrane. There are several effects through the LDPE coating layer on the PTFE HF membrane such as wettability resistance of membrane, surface roughness, thermal conductivity, and mass and heat transfer resistance. From Figure 6, the coating can effectively create a rough surface that affects the convection heat transfer and the Nusselt number with low Reynolds number, especially under a laminar flow.[56,57] Moreover, the hydrophobic layer is enhanced with the LDPE coating that inhibits liquid film appearance along

https://dx.doi.org/10.1021/acsomega.0c05107
ACS Omega 2021, 6, 4609−4618

Table 2. Summary of Works on Other Modified Membranes[a]

membrane	surface modification material	membrane properties upon modifications	flux (L m^{-2} h^{-1})	rejection (%)	ref
PTFE	spray coating with iron oxide carbon nanotube	WCA: 128 ± 1.8° porosity: not available pore size: 0.2 μm LEP: >3 bar	4	99.9	52
PP	coating with 1*H*,1*H*,2*H*,2*H*-perfluorooctyltriethoxysilane (POTS)	WCA: 157° porosity: 47.63% pore size: 0.0695 μm LEP: not available	1.2	99.8	53
PVDF	silane grafting with (tridecafluro-1,1,2,2-tetrahydrooctyl)triethoxysilane	WCA: >150° porosity: 56.4% pore size: 0.47 μm LEP: 0.5 bar	6	99.9	9
PES	surface grafting with tetraethylorthosilicate (TEOS) and trimethylchlorosilane (TMSCl)	WCA: 150° porosity: 84% pore size: not available LEP: not available	1.9	99.7	54
PET	photo-induced graft polymerization with triethoxyvinylsilane	WCA: 104° porosity: 5% pore size: 0.18 μm LEP: >4.3	0.7	99.3	55
PTFE	low-density polyethylene (LDPE) solution coating	WCA: 135.14 ± 0.24° porosity: 60.18 ± 0.10% pore size: 0.2 μm LEP: 0.9860 ± 0.02	4.12	99.9	this study

[a]PTFE, polytetrafluoroethylene; PVDF, polyvinylidene fluoride; PP, polypropylene; PES, polyethersulfone; and PET, polyethylene terephthalate.

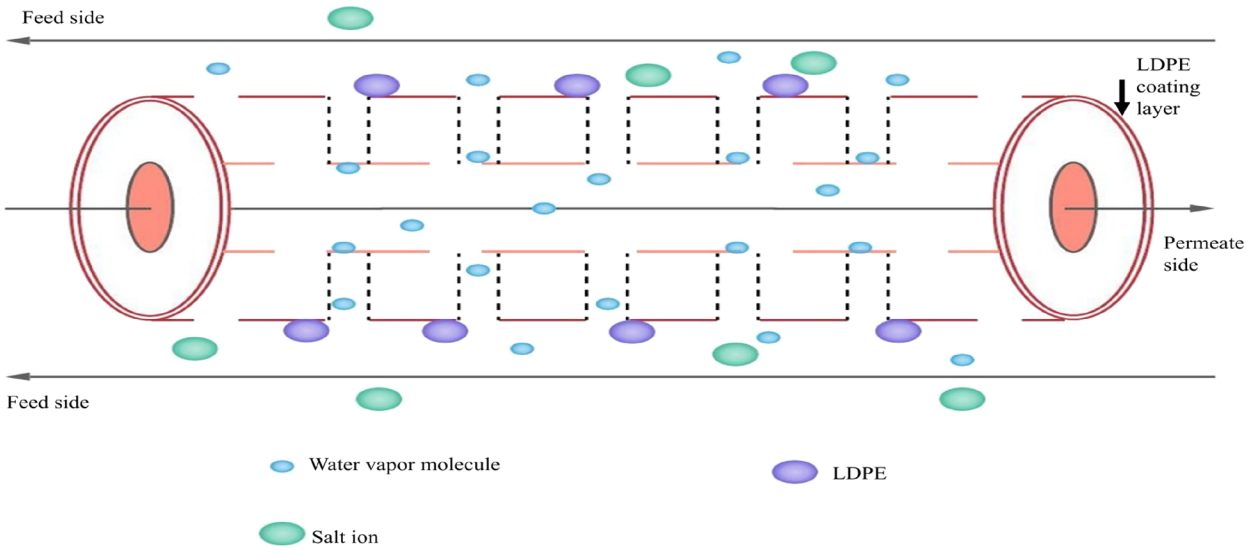

Figure 6. Schematic diagram of the effect of LDPE coating layer on the mass transfer of PTFE HF membrane.

with the outer PTFE HF membrane and gradually decreases the thickness of the boundary layer of temperature polarization.[58] Studies by Liu et al.[59] and He et al.[60] attributed high hydrophobicity and surface area to cause effective gas and vapor adsorption properties. Activated diffusion[61] from Figure 6 occurred when water molecules and salt ions come into contact with LDPE, where they will only allow vapor molecules to transport into the micropores of the PTFE membrane. Thus, the conductivity of salt ions at the permeate tank during the DCMD experiment decreases from 42.25 mS cm^{-1} to 6.819 μS cm^{-1}. Based on the above discussion, increased LDPE concentration can enhance membrane permeation flux compared to the uncoated PTFE HF membrane.

3. CONCLUSIONS

In this study, low-density polyethylene (LDPE) is used in the surface modification of polytetrafluorethylene (PTFE) HF membrane as the solution coating and proved to successfully enhance the hydrophobicity of the membrane surface and can be applied in direct contact to the membrane distillation (DCMD) process for desalination. At first, characterization analysis such as water contact angle, surface morphology, LEP, porosity, and FTIR was being put on a total focus. Later,

https://dx.doi.org/10.1021/acsomega.0c05107
ACS Omega 2021, 6, 4609−4618

detailed discussions on coated membranes for application of DCMD were presented. The LDPE concentrations (30 g/L) M-3 and (40 g/L) M-4 in the coating solution were found to produce favorable characteristics: high LEP (0.9868 and 0.9945 bar) and more hydrophobic (135.14 and 138.08°), respectively, compared to the pristine PTFE HF membrane (104.39°) and less reduction in porosity due to a thick LDPE layer cover on the membrane surface. The formation of a fine nanostructure on the membrane surface took place, which created a hydrophobic layer, a high roughness of membrane, and a buildup uniform LDPE network. In terms of the desalination test, all membranes showed high salt rejection with excellent removal of 99%. M-3 and M-4 are among the highest consistent flux readings of about 4.12 and 3.3 L m^{-2} h^{-1}, respectively, at 70 °C. A further decrease in water permeation flux of 1.95 L m^{-2} h^{-1} for M-5 was recorded when LDPE concentration increased. We believe that high concentration of LDPE coated on the layer of PTFE HF membrane causes reduction on membrane porosity and may eventually lead to high mass transfer resistance that could ultimately result in low water permeation flux.

4. EXPERIMENTAL SECTION

4.1. Materials. The polytetrafluoroethylene (PTFE) HF membranes with a size of 0.8 mm outer diameter (OD)/0.5 mm inner diameter (ID) and 0.2 μm pore size were purchased from PLC Solution (Malaysia). The low-density polyethylene (LDPE) commercial-grade pellets produced by Petlin Sdn. Bhd. (Malaysia) were used in this work. The polymer solvent used was xylene (>98.5 percent of the mixture isomers + ethyl benzene base, France) supplied by Sigma-Aldrich Sdn. Bhd. Ethanol (>99.9 percent, Germany) and a nonsolvent indirect coating were purchased from Merck Sdn. Bhd, while sodium chloride (NaCl) was purchased from Sigma-Aldrich (St. Louis, MO, USA) to be used as a feed solution.

4.2. Preparation of the LDPE Coating Solution. The LDPE coating solution was prepared according to the literature with some modifications.[51] The LDPE pellet was dried for 24 h in an oven at 60 °C and then slowly dissolved in xylene without further treatment at 85 °C. The pellets and the solvent were placed under continuous stirring at 300 rpm in a double jacket heating tank for 2 h until the polymer is completely dissolved. The above steps were repeated to study the effect of LDPE polymer concentration on membrane wettability according to Table 3.

Table 3. LDPE Polymer Concentration

PTFE HF membrane	LDPE polymer concentration (g/l)	mass of LDPE pellets (g)	mass of xylene (g)
M-0	pristine		
M-1	10	0.5	43.05
M-2	20	1.0	43.05
M-3	30	1.5	43.05
M-4	40	2.0	43.05
M-5	50	2.5	43.05

4.3. Modification of PTFE Hollow Fiber Membrane. PTFE HF membranes of 3 cm length were washed with distilled water and then rinsed with ethanol to remove contaminants from their surface. The fiber was then dried in the oven at 70 °C for 24 h, while at one end, the fibers were sealed with epoxy (Araldite, Hustsman Advance Materials, Belgium) to prevent the coating solution from flowing within the fiber lumen. The membrane was coated via indirect methods. The fiber was first immersed in nonsolvent solution (ethanol) for 30 s followed by 10 s in LDPE solution and dried at room temperature in a vacuum oven.

4.4. Characterization of LDPE Coating Layer. The coated LDPE on membrane surfaces was characterized based on surface morphology, wettability, Fourier transform infrared (FTIR), porosity, and liquid entry pressure (LEP).

4.4.1. Surface Morphology Checking. For morphology observation, the membranes were examined by scanning electron microscopy (SEM) using a Hitachi TM-3000 tabletop to study the morphology on the flat and curved surfaces of the fabricated LDPE layer. The membrane samples were coated with a conducting layer of gold and finally being observed by SEM.

4.4.2. Fourier Transform Infrared (FTIR). Polymer crystallinity checking by Fourier transform infrared spectroscopy or FTIR (Thermo Scientific, Nicolet iS10, USA) was conducted to identify the functional group of the pristine and modified membrane. The peaks represent PTFE and LDPE with different crystallinities. Data were collected in transmission mode after the membrane undergoes 32 scans within the wavenumber 4000−400 cm^{-1} at a resolution of 2 cm^{-1}.

4.4.3. Membrane Wettability Measurement. The membrane water contact angle (CA) was evaluated via goniometer equipment, Rame-Hart 250-F1 USA, based on the sessile drop method at ambient temperature. DI water (2 μL) was dropped through a micro syringe on the hollow fiber membrane surfaces. Then, a microscope was used to capture the micrographs. To determine the average and remove any occurring errors, this step was repeated for five surface measurements at different locations for each sample.

4.4.4. Porosity Measurement. The total porosity of pristine and modified HF membranes was calculated by the gravimetric method mentioned in the literature.[62] Three HF membranes of 3 cm long were used for each measurement to reduce error. The total porosity was averaged for three fibers and calculated according to the eq 4:

$$\varepsilon(\%) = \frac{[(W_w - W_d)/\rho_w] - [\pi r^2 h_f]}{[(W_w - W_d)/\rho_w] - [\pi r^2 h_f] + W_d/\rho_p} \times 100\% \quad (4)$$

where W_w and W_d are the weights of wet and dry membranes (g), ρ_w is the density of porefil (1.78 g/cm^3), r is the inner radius (cm), h_f is the length of fiber (1 cm), and ρ_p is the polymer density (2.2 g/cm^3).

4.4.5. Liquid Entry Pressure (LEP). Liquid entry pressure (LEP) is defined by the minimum pressure at which the first drop of the feed solution occurs on the fiber lumen side. In this work, HF membranes were equipped with water inserted in the lumen shell side in a stainless steel tubular module. The compressed nitrogen gas was added progressively and continuously (at a linear rate of 5 kPa for every 5 min) to the wetting liquid in contact with the membrane until the first drop of water on the permeated side.

4.4.6. Direct Contact Membrane Distillation (DCMD) Experiments. DCMD studies have been performed to determine the separation performance of various LDPE concentrations on the hollow fiber membrane surface (M-0, M-1, M-2, M-3, M-4, and M-5) and are illustrated in Figure 7. For each MD experiment, the HF membrane's effective length

https://dx.doi.org/10.1021/acsomega.0c05107
ACS Omega 2021, 6, 4609−4618

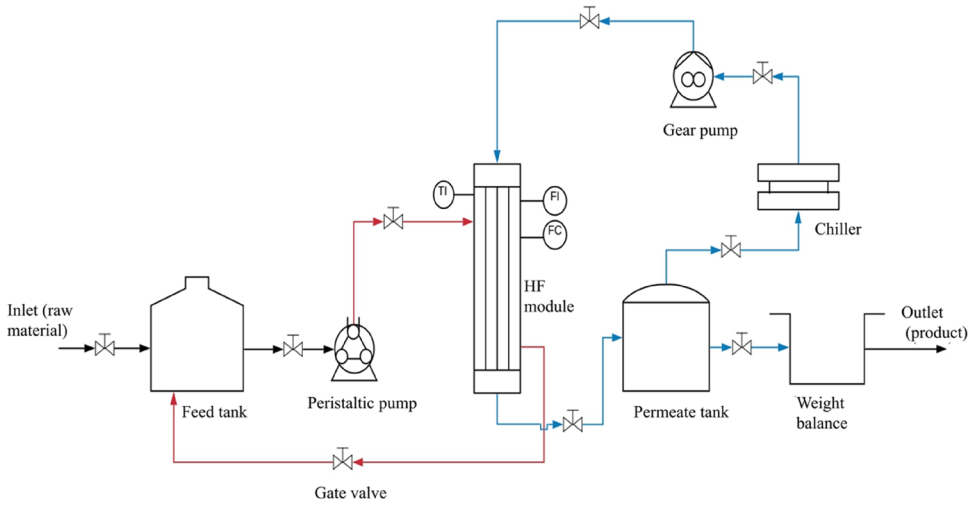

Figure 7. Schematic diagram of the DCMD test rig.

was estimated to be 28 cm long. DCMD tests were performed using 35 g/L sodium chloride (NaCl) to simulate seawater and heated at 70 °C by placing it in a hot water bath (Protech HC-10), whereas distilled water was maintained at 20 °C and used as a permeate circulated counter-currently using a gear pump. The feed solution (initial conductivity about 42.25mS cm^{-1}) was circulated on the shell side using a peristaltic pump, and meanwhile, water vapors penetrated through the micropores of the membrane and converged in the lumen fiber. The permeate flux (L m^{-2} h^{-1}) and salt rejection (%) of the membrane by MD were determined by eqs 5 and 6, respectively,

$$J = \frac{\Delta V}{A\Delta t} \tag{5}$$

$$R\ (\%) = \left[1 - \frac{C_p}{C_f}\right] \times 100 \tag{6}$$

where J is the permeate flux (L m^{-2} h^{-1}), ΔV is the quantity of volume distillate (L), A is the outer surface area of PTFE HF membrane (m^2), Δt is the time interval (h), R is the rejection coefficient (%), and C_p and C_f are the concentrations of NaCl (gL^{-1}) at permeate and feed, respectively. To evaluate the membrane efficiency, the membrane feed with distilled water was first run for 6 h then followed by NaCl for another 6 h.

AUTHOR INFORMATION

Corresponding Author

Abdul Latif Ahmad − *School of Chemical Engineering, Engineering Campus, Universiti Sains Malaysia, Seberang Perai Selatan, Pulau Pinang 14300, Malaysia;* orcid.org/0000-0003-1612-3032; Email: chlatif@usm.my

Authors

Mohamad Razif Mohd Ramli − *School of Chemical Engineering, Engineering Campus, Universiti Sains Malaysia, Seberang Perai Selatan, Pulau Pinang 14300, Malaysia*

Choe Peng Leo − *School of Chemical Engineering, Engineering Campus, Universiti Sains Malaysia, Seberang Perai Selatan, Pulau Pinang 14300, Malaysia;* orcid.org/0000-0002-5664-6412

Complete contact information is available at: https://pubs.acs.org/10.1021/acsomega.0c05107

Notes

The authors declare no competing financial interest.

ACKNOWLEDGMENTS

The authors would like to acknowledge the financial support to M.R.M.R. by Universiti Sains Malaysia under the fellowship scheme. This study was funded by the Ministry of Higher Education of Malaysia for the Long Term Research Grant Scheme 1/2018, LRGS (203/PJKIMIA/67215002) and USM-rui Grant (10001.PJKIMIA.8014063).

REFERENCES

(1) Chung, H. J.; Kim, J.; Kim, D. I.; Gwak, G.; Hong, S. Feasibility Study of Reverse Osmosis−flow Capacitive Deionization (RO-FCDI) for Energy-Efficient Desalination Using Seawater as the Flow-Electrode Aqueous Electrolyte. *Desalination* **2020**, *479*, 114326.

(2) Wei, Q. J.; Tucker, C. I.; Wu, P. J.; Trueworthy, A. M.; Tow, E. W.; Lienhard, J. H. Impact of Salt Retention on True Batch Reverse Osmosis Energy Consumption: Experiments and Model Validation. *Desalination* **2020**, *479*, 114177.

(3) El-Bourawi, M. S.; Ding, Z.; Ma, R.; Khayet, M. A Framework for Better Understanding Membrane Distillation Separation Process. *J. Membr. Sci.* **2006**, *285*, 4−29.

(4) Shaulsky, E.; Karanikola, V.; Straub, A. P.; Deshmukh, A.; Zucker, I.; Elimelech, M. Asymmetric Membranes for Membrane Distillation and Thermo-Osmotic Energy Conversion. *Desalination* **2019**, *452*, 141−148.

(5) Laqbaqbi, M.; García-Payo, M. C.; Khayet, M.; El Kharraz, J.; Chaouch, M. Application of Direct Contact Membrane Distillation for Textile Wastewater Treatment and Fouling Study. *Sep. Purif. Technol.* **2019**, *209*, 815−825.

(6) Mokhtar, N. M.; Lau, W. J.; Ismail, A. F.; Veerasamy, D. Membrane Distillation Technology for Treatment of Wastewater from Rubber Industry in Malaysia. *Procedia CIRP* **2015**, *26*, 792−796.

(7) Reis, B. G.; Araújo, A. L. B.; Amaral, M. C. S.; Ferraz, H. C. Comparison of Nanofiltration and Direct Contact Membrane Distillation as an Alternative for Gold Mining Effluent Reclamation. *Chem. Eng. Process.* **2018**, *133*, 24−33.

(8) Rao, U.; Posmanik, R.; Hatch, L. E.; Tester, J. W.; Walker, S. L.; Barsanti, K. C.; Jassby, D. Coupling Hydrothermal Liquefaction and Membrane Distillation to Treat Anaerobic Digestate from Food and Dairy Farm Waste. *Bioresour. Technol.* **2018**, *267*, 408−415.

(9) Hamzah, N.; Leo, C. P. Membrane Distillation of Saline with Phenolic Compound Using Superhydrophobic PVDF Membrane Incorporated with TiO2 Nanoparticles: Separation, Fouling and Self-Cleaning Evaluation. *Desalination* **2017**, *418*, 79−88.

https://dx.doi.org/10.1021/acsomega.0c05107
ACS Omega 2021, 6, 4609−4618

(10) Guo, J.; Farid, M. U.; Lee, E.-J.; Yan, D. Y.-S.; Jeong, S.; Kyoungjin An, A. Fouling Behavior of Negatively Charged PVDF Membrane in Membrane Distillation for Removal of Antibiotics from Wastewater. *J. Membr. Sci.* **2018**, *551*, 12−19.
(11) Zhang, P.; Knötig, P.; Gray, S.; Duke, M. Scale Reduction and Cleaning Techniques during Direct Contact Membrane Distillation of Seawater Reverse Osmosis Brine. *Desalination* **2015**, *374*, 20−30.
(12) Kang, G.-d.; Cao, Y.-m. Application and ModifiCation of Poly(Vinylidene Fluoride)(PVDF) Membranes − A Review. *J. Membr. Sci.* **2014**, *463*, 145−165.
(13) Alklaibi, A. M.; Lior, N. Comparative Study of Direct-Contact and Air-Gap Membrane Distillation Processes. *Ind. Eng. Chem. Res.* **2007**, *46*, 584−590.
(14) Bamasag, A.; Alqahtani, T.; Sinha, S.; Ghaffour, N.; Phelan, P. Experimental Investigation of a Solar-Heated Direct Contact Membrane Distillation System Using Evacuated Tube Collectors. *Desalination* **2020**, *487*, 114497.
(15) Criscuoli, A.; Drioli, E. Date Juice Concentration by Vacuum Membrane Distillation. *Sep. Purif. Technol.* **2020**, *251*, 117301.
(16) Narayan, A.; Pitchumani, R. Analysis of an Air-Cooled Air Gap Membrane Distillation Module. *Desalination* **2020**, *475*, 114179.
(17) Said, I. A.; Chomiak, T.; Floyd, J.; Li, Q. Sweeping Gas Membrane Distillation (SGMD) for Wastewater Treatment, Concentration, and Desalination: A Comprehensive Review. *Chem. Eng. Process.* **2020**, *153*, 107960.
(18) Ashoor, B. B.; Mansour, S.; Giwa, A.; Dufour, V.; Hasan, S. W. Principles and Applications of Direct Contact Membrane Distillation (DCMD): A Comprehensive Review. *Desalination* **2016**, *398*, 222−246.
(19) Teoh, G. H.; Chin, J. Y.; Ooi, B. S.; Jawad, Z. A.; Leow, H. T. L.; Low, S. C. Superhydrophobic Membrane with Hierarchically 3D-Microtexture to Treat Saline Water by Deploying Membrane Distillation. *J. Water Process Eng.* **2020**, *37*, 101528.
(20) Guillen-Burrieza, E.; Servi, A.; Lalia, B. S.; Arafat, H. A. Membrane Structure and Surface Morphology Impact on the Wetting of MD Membranes. *J. Membr. Sci.* **2015**, *483*, 94−103.
(21) Tibi, F.; Charfi, A.; Cho, J.; Kim, J. Fabrication of Polymeric Membranes for Membrane Distillation Process and Application for Wastewater Treatment: Critical Review. *Process Saf. Environ. Prot.* **2020**, *141*, 190−201.
(22) Teoh, M. M.; Chung, T.-S. Membrane Distillation with Hydrophobic Macrovoid-Free PVDF−PTFE Hollow Fiber Membranes. *Sep. Purif. Technol.* **2009**, *66*, 229−236.
(23) Figoli, A.; Ursino, C.; Galiano, F.; Di Nicolò, E.; Campanelli, P.; Carnevale, M. C.; Criscuoli, A. Innovative Hydrophobic Coating of Perfluoropolyether (PFPE) on Commercial Hydrophilic Membranes for DCMD Application. *J. Membr. Sci.* **2017**, *522*, 192−201.
(24) Rajwade, K.; Barrios, A. C.; Garcia-Segura, S.; Perreault, F. Pore Wetting in Membrane Distillation Treatment of Municipal Wastewater Desalination Brine and Its Mitigation by Foam Fractionation. *Chemosphere* **2020**, *257*, 127214.
(25) Rezaei, M.; Warsinger, D. M.; Lienhard, J. H.; Duke, M. C.; Matsuura, T.; Samhaber, W. M. Wetting Phenomena in Membrane Distillation: Mechanisms, Reversal, and Prevention. *Water Res.* **2018**, *139*, 329−352.
(26) Kuang, Z.; Long, R.; Liu, Z.; Liu, W. Analysis of Temperature and Concentration Polarizations for Performance Improvement in Direct Contact Membrane Distillation. *Int. J. Heat Mass Transfer* **2019**, *145*, 118724.
(27) Abu-zeid, M. A. E.-R.; Zhang, Y.; Dong, H.; Zhang, L.; Chen, H.-L.; Hou, L. A Comprehensive Review of Vacuum Membrane Distillation Technique. *Desalination* **2015**, *356*, 1−14.
(28) Horseman, T.; Su, C.; Christie, K. S. S.; Lin, S. Highly Effective Scaling Mitigation in Membrane Distillation Using a Superhydrophobic Membrane with Gas Purging. *Environ. Sci. Technol. Lett.* **2019**, *6*, 423−429.
(29) Ahmad, A. L.; Ramli, M. R. M.; Esham, M. I. M. Effect of Additives on Hydrophobicity of PVDF Membrane in Two-Stage Coagulation Baths for Desalination. *J. Phys. Sci.* **2019**, *30*, 207−221.
(30) Meng, S.; Ye, Y.; Mansouri, J.; Chen, V. Fouling and Crystallisation Behaviour of Superhydrophobic Nano-Composite PVDF Membranes in Direct Contact Membrane Distillation. *J. Membr. Sci.* **2014**, *463*, 102−112.
(31) Alsebaeai, M. K.; Ahmad, A. L. Membrane Distillation: Progress in the Improvement of Dedicated Membranes for Enhanced Hydrophobicity and Desalination Performance. *J. Ind. Eng. Chem.* **2020**, *86*, 13−34.
(32) Li, X.; Chen, G.; Ma, Y.; Feng, L.; Zhao, H.; Jiang, L.; Wang, F. Preparation of a Super-Hydrophobic Poly(vinyl Chloride) Surface via Solvent−nonsolvent Coating. *Polymer* **2006**, *47*, 506−509.
(33) Chen, H.; Yuan, Z.; Zhang, J.; Liu, Y.; Li, K.; Zhao, D.; Li, S.; Shi, P.; Tang, J. Preparation, Characterization and Wettability of Porous Superhydrophobic Poly (Vinyl Chloride) Surface. *J. Porous Mater.* **2009**, *16*, 447−451.
(34) Ahmad, A. L.; Mohammed, H. N.; Ooi, B. S.; Leo, C. P. Deposition of a Polymeric Porous Superhydrophobic Thin Layer on the Surface of Poly(vinylidenefluoride) Hollow Fiber Membrane. *Polish J. Chem. Technol.* **2013**, *15*, 1−6.
(35) Lu, X.; Zhang, C.; Han, Y. Low-Density Polyethylene Superhydrophobic Surface by Control of Its Crystallization Behavior. *Macromol. Rapid Commun.* **2004**, *25*, 1606−1610.
(36) Wenzel, R. N. RESISTANCE OF SOLID SURFACES TO WETTING BY WATER. *Ind. Eng. Chem.* **1936**, *28*, 988−994.
(37) Liao, Y.; Wang, R.; Fane, A. G. Engineering Superhydrophobic Surface on Poly(vinylidene Fluoride) Nanofiber Membranes for Direct Contact Membrane Distillation. *J. Membr. Sci.* **2013**, *440*, 77−87.
(38) Bux, H.; Liang, F.; Li, Y.; Cravillon, J.; Wiebcke, M.; Caro, J. Zeolitic Imidazolate Framework Membrane with Molecular Sieving Properties by Microwave-Assisted Solvothermal Synthesis. *J. Am. Chem. Soc.* **2009**, *131*, 16000−16001.
(39) Khayet, M.; Essalhi, M.; Qtaishat, M. R.; Matsuura, T. Robust Surface Modified Polyetherimide Hollow Fiber Membrane for Long-Term Desalination by Membrane Distillation. *Desalination* **2019**, *466*, 107−117.
(40) Dong, Z.-Q.; Ma, X.-h.; Xu, Z.-L.; You, W.-T.; Li, F.-b. Superhydrophobic PVDF−PTFE Electrospun Nanofibrous Membranes for Desalination by Vacuum Membrane Distillation. *Desalination* **2014**, *347*, 175−183.
(41) Saffarini, R. B.; Mansoor, B.; Thomas, R.; Arafat, H. A. Effect of Temperature-Dependent Microstructure Evolution on Pore Wetting in PTFE Membranes under Membrane Distillation Conditions. *J. Membr. Sci.* **2013**, *429*, 282−294.
(42) Choi, W.; Tuteja, A.; Mabry, J. M.; Cohen, R. E.; McKinley, G. H. A Modified Cassie−Baxter Relationship to Explain Contact Angle Hysteresis and Anisotropy on Non-Wetting Textured Surfaces. *J. Colloid Interface Sci.* **2009**, *339*, 208−216.
(43) Fazullin, D. D.; Mavrin, G. V.; Sokolov, M. P.; Shaikhiev, I. G. Infrared Spectroscopic Studies of the PTFE and Nylon Membranes Modified Polyaniline. *Mod. Appl. Sci.* **2014**, *9*, 242−249.
(44) Rogachev, A. A.; Tamulevičius, S.; Rogachev, A. V.; Yarmolenko, M. A.; Prosycevas, I. The Structure and Molecular Orientation of Polytetrafluoroethylene Coatings Deposited from Active Gas Phase. *Appl. Surf. Sci.* **2009**, *255*, 6851−6856.
(45) Henda, R.; Wilson, G.; Gray-Munro, J.; Alshekhli, O.; McDonald, A. M. Preparation of Polytetrafluoroethylene by Pulsed Electron Ablation: Deposition and Wettability Aspects. *Thin Solid Films* **2012**, *520*, 1885−1889.
(46) Grant Norton, M.; Jiang, W.; Thomas Dickinson, J.; Hipps, K. W. Pulsed Laser Ablation and Deposition of Fluorocarbon Polymers. *Appl. Surf. Sci.* **1996**, *96-98*, 617−620.
(47) Kwong, H. Y.; Wong, M. H.; Wong, Y. W.; Wong, K. H. Superhydrophobicity of Polytetrafluoroethylene Thin Film Fabricated by Pulsed Laser Deposition. *Appl. Surf. Sci.* **2007**, *253*, 8841−8845.
(48) Wang, S.; Li, J.; Suo, J.; Luo, T. Surface Modification of Porous Poly(tetrafluoraethylene) Film by a Simple Chemical Oxidation Treatment. *Appl. Surf. Sci.* **2010**, *256*, 2293−2298.

https://dx.doi.org/10.1021/acsomega.0c05107
ACS Omega 2021, 6, 4609−4618

(49) Ferkany, J. W. Molecular Biology and Biotechnology. A Comprehensive Desk Reference Edited by Robert A. Meyers. VCH Publishers. New York. 1995. xxxviii + 1034 pp. 21.5 × 27.5 cm. ISBN 1-56081-925-1. $59.95. *J. Med. Chem.* **1996**, *39*, 1565−1566.
(50) Gulmine, J. V.; Janissek, P. R.; Heise, H. M.; Akcelrud, L. Polyethylene Characterization by FTIR. *Polym. Test.* **2002**, *21*, 557−563.
(51) Rosli, A.; Ahmad, A. L.; Low, S. C. Anti-Wetting Polyvinylidene Fluoride Membrane Incorporated with Hydrophobic Polyethylene-Functionalized-Silica to Improve CO_2 Removal in Membrane Gas Absorption. *Sep. Purif. Technol.* **2019**, *221*, 275−285.
(52) Anvari, A.; Kekre, K. M.; Yancheshme, A. A.; Yao, Y.; Ronen, A. Membrane Distillation of High Salinity Water by Induction Heated Thermally Conducting Membranes. *J. Membr. Sci.* **2019**, *589*, 117253.
(53) Xu, Z.; Liu, Z.; Song, P.; Xiao, C. Fabrication of Super-Hydrophobic Polypropylene Hollow Fiber Membrane and Its Application in Membrane Distillation. *Desalination* **2017**, *414*, 10−17.
(54) Rastegarpanah, A.; Mortaheb, H. R. Surface Treatment of Polyethersulfone Membranes for Applying in Desalination by Direct Contact Membrane Distillation. *Desalination* **2016**, *377*, 99−107.
(55) Korolkov, I. V.; Gorin, Y. G.; Yeszhanov, A. B.; Kozlovskiy, A. L.; Zdorovets, M. V. Preparation of PET Track-Etched Membranes for Membrane Distillation by Photo-Induced Graft Polymerization. *Mater. Chem. Phys.* **2018**, *205*, 55−63.
(56) Lee, J.-G.; Lee, E.-J.; Jeong, S.; Guo, J.; An, A. K.; Guo, H.; Kim, J.; Leiknes, T. O.; Ghaffour, N. Theoretical Modeling and Experimental Validation of Transport and Separation Properties of Carbon Nanotube Electrospun Membrane Distillation. *J. Membr. Sci.* **2017**, *526*, 395−408.
(57) Kandlikar, S. G.; Joshi, S.; Tian, S. Effect of Surface Roughness on Heat Transfer and Fluid Flow Characteristics at Low Reynolds Numbers in Small Diameter Tubes. *Heat Transfer Eng.* **2010**, *24*, 4−16.
(58) Drioli, E.; Ali, A.; Simone, S.; Macedonio, F.; AL-Jlil, S. A.; Al Shabonah, F. S.; Al-Romaih, H. S.; Al-Harbi, O.; Figoli, A.; Criscuoli, A. Novel PVDF Hollow Fiber Membranes for Vacuum and Direct Contact Membrane Distillation Applications. *Sep. Purif. Technol.* **2013**, *115*, 27−38.
(59) Liu, S.; Liu, G.; Zhao, X.; Jin, W. Hydrophobic-ZIF-71 Filled PEBA Mixed Matrix Membranes for Recovery of Biobutanol via Pervaporation. *J. Membr. Sci.* **2013**, *446*, 181−188.
(60) He, H.; Hashemi, L.; Hu, M.-L.; Morsali, A. The Role of the Counter-Ion in Metal-Organic Frameworks' Chemistry and Applications. *Coord. Chem. Rev.* **2018**, *376*, 319−347.
(61) Li, H.; Shi, W.; Zeng, X.; Huang, S.; Zhang, H.; Qin, X. Improved Desalination Properties of Hydrophobic GO-Incorporated PVDF Electrospun Nanofibrous Composites for Vacuum Membrane Distillation. *Sep. Purif. Technol.* **2020**, *230*, 115889.
(62) Ahmad, A. L.; Pang, W. Y.; Mohd Shafie, Z. M. H.; Zaulkiflee, N. D. PES/PVP/TiO 2 Mixed Matrix Hollow Fiber Membrane with Antifouling Properties for Humic Acid Removal. *J. Water Process Eng.* **2019**, *31*, 100827.

https://dx.doi.org/10.1021/acsomega.0c05107
ACS Omega 2021, 6, 4609−4618